buildings

MDPI

Article

Development and Investigation of Repair Self-Sensing Composites Using S-CNT

Youngmin Kim [1], Soo-Yeon Seo [1], Hyun-Do Yun [2], Gun-Cheol Lee [1,*] and Seongwon Hong [3,*]

[1] Department of Architectural Engineering, Korea National University of Transportation, Chungju-si 27469, Republic of Korea
[2] Department of Architectural Engineering, Chungnam National University, Daejeon 34134, Republic of Korea
[3] Department of Safety Engineering, Korea National University of Transportation, Chungju-si 27469, Republic of Korea
* Correspondence: gclee@ut.ac.kr (G.-C.L.); shong@ut.ac.kr (S.H.); Tel.: +82-43-841-5207 (G.-C.L.); +82-43-841-5339 (S.H.)

Abstract: This study analyzed the mechanical and electrical characteristics of repair self-sensing composites. In order to ensure homogeneous dispersion of carbon nanotubes (CNTs) in the repair mortar, porous powder was impregnated with the liquid MWCNT, dried, and then pulverized. This CNT powder was named S-CNT, and a repair self-sensing cement composite was fabricated using it with different dosages, by weight, of 3, 6, and 9%. Mechanical and electrical performances of the developed materials were investigated through flexural, compressive, and bonding strengths, dry shrinkage, porosity, and fractional change in resistance (FCR) tests. There was little difference in terms of strength, between the three different composites made with the different dosages of S-CNT. The strength of the composite with 9% of S-CNT was even higher than that of the plain specimen. As a result of measuring drying shrinkage, conducted to evaluate the effect of improving dispersion, the length change rate decreased as the amount of S-CNT increased. As a result of the porosity results of the specimens incorporating the same mass of CNT as S-CNT, it was confirmed that the dispersibility was clearly improved. In addition, as an electrical characteristic, when the S-CNT mixed specimen was repeatedly loaded with a bending load, FCR appeared, confirming the self-sensing performance.

Keywords: carbon nanotube; impregnation; S-CNT; porous powder; self-sensing; repair

Citation: Kim, Y.; Seo, S.-Y.; Yun, H.-D.; Lee, G.-C.; Hong, S. Development and Investigation of Repair Self-Sensing Composites Using S-CNT. *Buildings* **2023**, *13*, 1015. https://doi.org/10.3390/buildings13041015

Academic Editors: Isabel Torres and Ana Luísa Velosa

Received: 7 March 2023
Revised: 3 April 2023
Accepted: 8 April 2023
Published: 12 April 2023

1. Introduction

Cement concrete is the most popular and widely used construction material in the world, due to its durability, versatility, availability, adaptability, high strength, and low cost. However, over time, structural components of buildings are constantly subjected to loads, and concrete building structures can suffer from diverse types of damage and degradation such as cracking, spalling, and corrosion, induced by internal or external environmental factors, resulting in significant reduction of their strength and service life. Currently, crack inspection and strength measurement through core sampling, are relied upon as methods for evaluating the performance degradation of building components. However, these methods are not suitable for immediate diagnosis of the building's condition, and can involve subjective judgment on the part of the inspector. Repairing damaged concrete building structures is essential for maintaining and improving their safety and durability. One of the key challenges in the concrete repair industry, is ensuring that the repaired structure has the same mechanical and physical properties as the original structure. In addition, it is important to monitor the condition of the repaired structure in order to detect any damage or degradation before it becomes severe.

Structural health monitoring (SHM) is an effective method that has been employed to detect, monitor, locate, and quantify damage and degradation in concrete structures [1–9]. SHM involves the use of various sensors to continuously monitor the structure's conditions, and provide real-time feedback on its health. This allows for early detection of any potential issues and problems, which can be addressed before they become critical. The development of self-sensing materials is a promising approach to SHM. Self-sensing materials such as graphite powder, steel slag, carbon fiber, carbon nanotube, and carbon block, or mixtures of such materials, have the ability to monitor their own condition and give information on the health of the structure [10–26]. In particular, carbon nanotubes (CNTs) have been extensively and thoroughly studied and used as self-sensing composites because of their exceptional mechanical and electrical properties. CNTs can be embedded into a concrete matrix to create a self-sensing capability that can detect changes in both mechanical and physical properties. However, the dispersion of CNTs in concrete is a critical issue that affects the performance of the composite. Grossiord et al. [27] used an ultrasonic disperser to ensure proper dispersion in cement mixtures. In research from Ma et al. [28], it was found that the vibration of an ultrasonic device caused increases in voids between hydration particles, resulting in homogeneous dispersion of CNT in the composites. According to Makar et al. [29], the most effective method to use in order to have uniform dispersion, was the use of ethanol and ultrasonic vibration. Konsta-Gdoutos et al. [30] conducted experiments using surfactants and ultrasonication to properly disperse CNTs in cement composites, and found that a minimum ultrasonic energy of 70 Pa was required in order to achieve uniform dispersion. Luo et al. [31] performed lab tests on cement pastes containing CNT dispersion solutions prepared using surfactants, and found that using surfactants significantly improved the compressive and flexural strengths. A scanning electron microscope (SEM) method was employed by Kim et al. [32] to observe the dispersion of CNTs in cementitious composites with silica fume, and it was worth noting that spherical silica fumes were still present in the mixtures after hydration, which filled the spaces of CNT agglomeration and ultimately resulted in agglomeration size reduction. Cwirzen et al. [33] found that CNTs modified with poly-acrylic polymer in an aqueous solution, were homogenously dispersed for more than two months. Nochaiya and Chaipanich [34] used mercury intrusion porosimetry and SEM to identify the behavior of CNTs in terms of porosity and microstructures, and concluded that the water-to-binder ratio greatly influenced the degree of dispersion in cement mixtures. Madenci et al. [35] performed mechanical tests using carbon nanotube reinforced textile-based composites. Despite the extensive research, studies, and investigations, there is a pressing need for research on self-sensing repair mortars for buildings requiring repair and reinforcement due to aging. Therefore, it is necessary to apply self-sensing repair mortars to existing components in need of repair, and to conduct research on their ability to endow buildings with self-sensing capabilities. In particular, there are few works on the use of a porous powder, zeolite, in achieving proper dispersion in self-sensing composites. Zeolite has been used to impregnate CNTs and improve their dispersion in a cementitious matrix.

The objective of this study is to develop a repair self-sensing composite that can be used for the effective repair and monitoring of damaged concrete structures. The mechanical and electrical performances of the composite were evaluated through various tests, including flexural, compressive, and bonding strengths, as well as dry shrinkage, porosity, and fractional change in resistance (FCR) tests. The results of these tests provide important information on the performance of the composite and its potential use in the repair and monitoring of concrete structures.

2. Test Program

Materials, Mixture Proportions, and Test Methods

In this study, Ordinary Portland Cement (Type I KS L 5201) was used as the cementitious material, and its chemical and physical properties are shown in Table 1. To fabricate self-sensing cementitious composites for repair, liquid-type multi-walled carbon nanotubes (MWCNTs, Kumho Petrochemical) were used, and their physical properties were summarized in Table 2 [36]. Since it was impossible to achieve uniform dispersion of MWCNTs in the composites, a porous material was employed.

Table 1. Chemical and physical properties of OPC.

Chemical Properties (%)					Physical Properties	
SiO_2	Al_2O_3	Fe_2O_3	CaO	MgO	Density (g/cm^3)	Fineness (cm^2/g)
22.2	5.2	3.4	64.6	2.3	3.15	3300

Table 2. Physical properties of MWCNT.

Item	MWCNT
Diameter (nm)	5~100
Length (μm)	10
Thermal conductivity (W/m·K)	Max. 3000
Tension (GPa)	<50
Electrical resistance ($\Omega \cdot m^2$)	5.1×10^{-6}
Specific surface area (m^2/g)	130~160

Figure 1 shows the impregnation process with MWCNT and a porous powder, zeolite. First, a 3% MWCNT dispersion was impregnated with porous powder, and dried at 60 °C for 48 h, crushed, and finally sieved through a No. 100 sieve (150 μm), to be used in powder form, called S-CNT. Figure 2 demonstrates SEM images of the S-CNT. It was clearly identified that there was fiber-type CNT hung on the surface of zeolite particles (see Figure 2a,b). The aggregate used in this study was silica sand, and the particle size distribution of the silica sand was summarized in Table 3. Aggregates were replaced with SCNT in terms of mass fraction, and only aggregates below 0.15 mm in size were replaced.

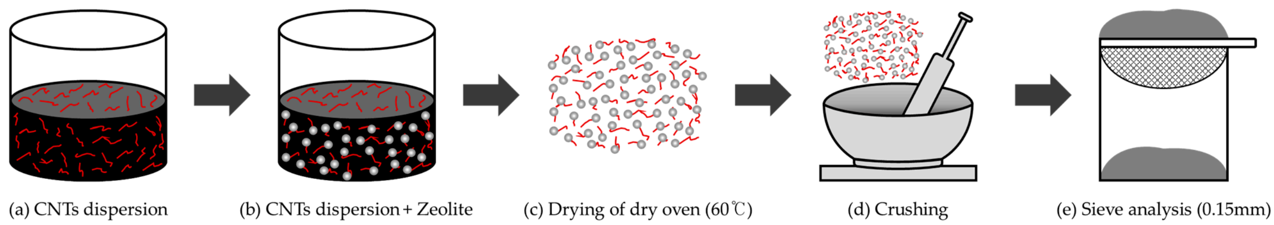

Figure 1. Impregnation process with MWCNTs and porous powder.

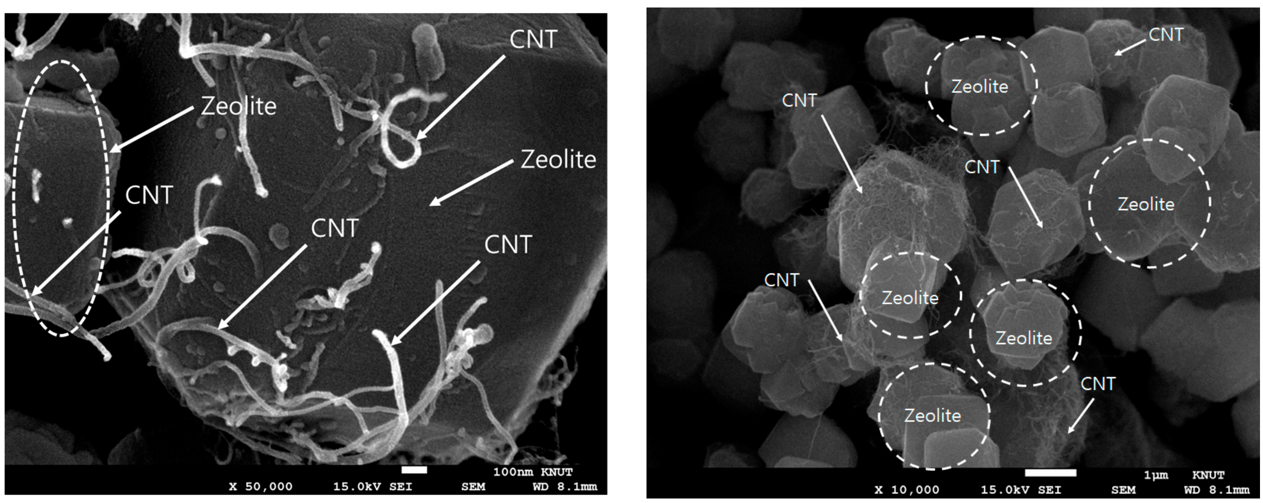

(**a**) magnification 50,000 × (**b**) magnification 10,000×

Figure 2. S-CNT SEM images: (**a**) magnification 50,000×; (**b**) magnification 10,000×.

Table 3. Particle size distribution of silica sand (mass fraction).

Specimen	Silica Sand (%)					S-CNT(%)
	2 mm	1.8 mm	0.9 mm	0.4 mm	0.15 mm	0.15 mm
PLAIN	10	10	40	30	10	0
SC3					7	3
SC6					4	6
SC9					1	9

Notes: SC3, 6, and 9 are 3, 6, and 9% of the silica sand replaced with SCNT, respectively.

A water-to-binder ratio (W/B) was set as 0.34. The polymer is a synthetic rubber-based resin, and the main purpose of adding the polymer was to improve the bonding strength in the repair mortar. The small amount of the poly carboxylate-based high-performance water reducing agent (KS F 2560) called chemical admixtures, was mixed into the repair self-sensing composites. Table 4 shows the mixture proportion by mass fraction.

Table 4. Mixture proportions (mass fraction).

Spec	W/B (%)	Binder (%)		Aggregate (%)		Admixture (%)
		Cement	Polymer	Silica Sand	S-CNT	
Plain	34	96	4	100	0	0.1
SC3				97	3	
SC6				94	6	
SC9				91	9	

According to KS F 2476, cement, polymer, silica sand, and S-CNT were dry mixed for 30 s, water was added to the mixture, and wet mixing was performed for 90 s. Flexural and compressive strength tests were conducted as per KS F 4042. The rectangular parallelepiped specimen was fabricated in the size of $40 \times 40 \times 160$ mm^3, and cured in a water tank at 20 ± 2 °C. The flexural strength of the specimen was measured at the ages of 3, 7, and 28 days, and the split specimens were employed to measure the compressive strength. Flexural and compressive strengths were determined by Equations (1) and (2), respectively.

$$\sigma_f = \frac{T}{1600} \tag{1}$$

where σ_f is flexural strength (N/mm^2), and T is maximum load (N).

$$\sigma_c = P \times 0.00234 \tag{2}$$

where σ_c is compressive strength (N/mm^2), and P is maximum load (N). To measure the bonding strength of repair cementitious composite, rectangular plate specimens with dimensions of $40 \times 40 \times 10$ mm^3 were fabricated according to KS L ISO 679, as displayed in Figure 3.

It was cured in an environmental chamber for 24 h at the temperature of 20 ± 2 °C and humidity of 80% or higher, and after de-molding, it was cured under the water tank for 6 days at the temperature of 20 ± 2 °C, and then further cured in the chamber at the temperature of 20 ± 2 °C and humidity of 60% or higher, for over 21 days. Bonding strength was calculated by Equation (3).

$$\sigma_b = \frac{T}{1600} \tag{3}$$

where σ_b is Bonding strength (N/mm^2), and T is maximum tensile load (N). A dry shrinkage test was carried out in accordance with KS F 2424. Rectangular parallelepiped specimens were made with a cross-section of 40×40 mm^2 and a length of 160 mm, demolded after 24 h, cured in a water tank maintained at 20 ± 2 °C for 5 days, and then further cured in the chamber at the temperature of 20 ± 2 °C and the humidity of 60%, until the target day. Figure 4 shows a cylindrical shaped specimen for the porosity test with a diameter of approximately 100 mm and a height of about 10 mm. To measure the pore size, the mercury intrusion porosimetry method was employed with the Autopore 9600IV (measurement range of 0.003–900 µm. ATS Scientific Inc., Burlington, ON, Canada). The sample was cured in a water tank for 28 days, and dried for 4 h at 50 °C.

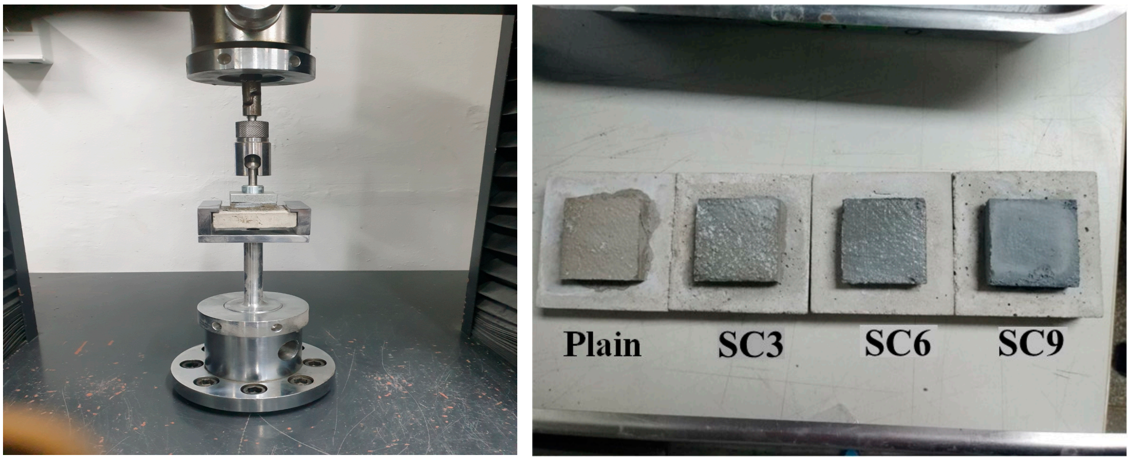

Figure 3. Bonding strength test.

Figure 4. Sample of repair cementitous composite for porosity.

Figure 5 presents the schematic of the fractional change in resistance (FCR) measurements during cyclic loading. The same size of rectangular parallelepiped specimen was fabricated, demolded 24 h after casting, and cured in the water tank at the temperature of 20 ± 2 °C, for 28 days. In order to minimize the water's effect on the resistance in the composite, the specimen was dried for 48 h at 50 °C. A 30% loading of the flexural strength was chosen as the cyclic loading level, and the FCR was calculated in Equation (4).

$$\mathrm{FCR} = \frac{R_n - R_0}{R_0} \tag{4}$$

where R_n is electrical resistance during loading (Ω), and R_0 is initial electrical resistance before loading (Ω). When measuring electrical resistance, in order to prevent polarization (increase in resistance value due to movement of electrons), after letting a current of 5 V flow for 1 h, the resistance value was then measured simultaneously with a load. To evaluate the repair performance of the cementitious composite, the plate specimen was made as per KS L ISO 69, as depicted in Figure 6a, and cured under water at 20 ± 2 °C for 28 days. After filling repair mortar, it was further cured in a water tank at a temperature of 20 ± 2 °C for 28 days, as shown in Figure 6b, and then its flexural strength was measured.

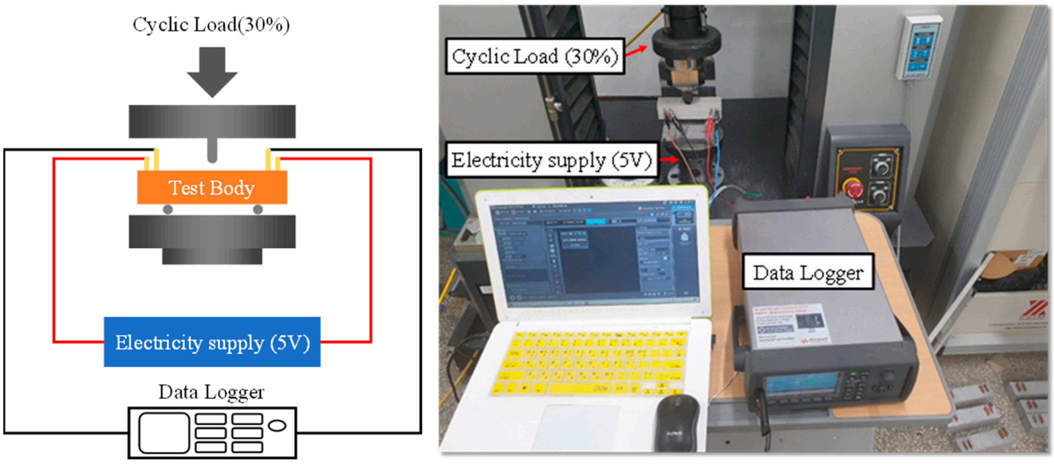

Figure 5. Schematic of fractional change in resistance measurement during cyclic loading.

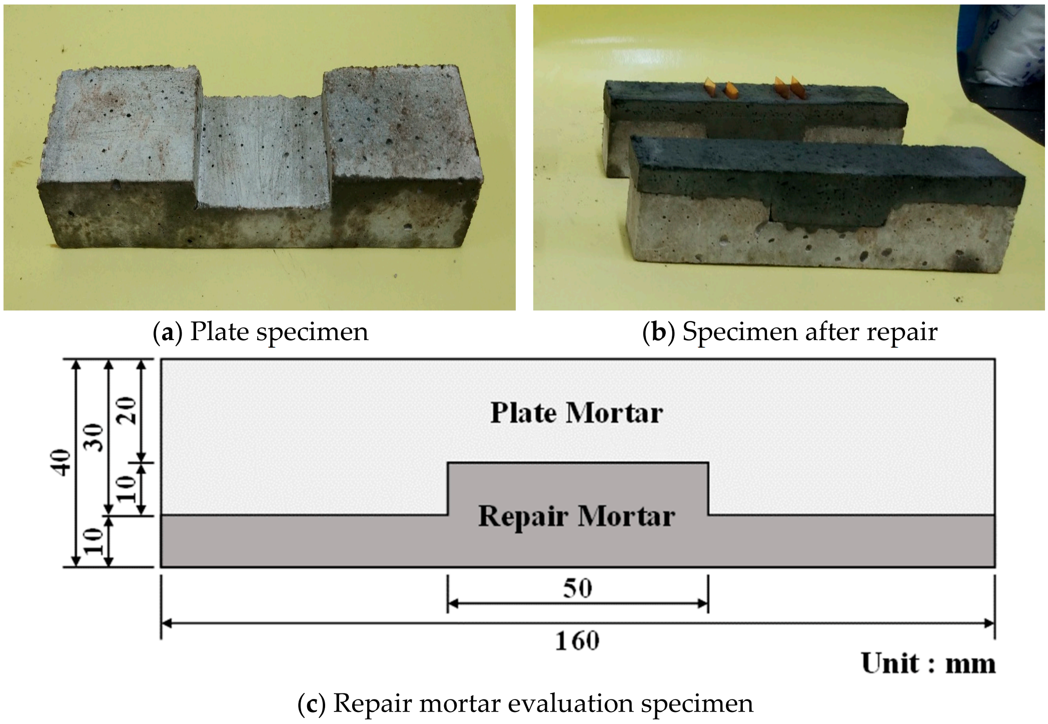

Figure 6. Flexural strength specimen after repair: (**a**) Plate specimen; (**b**) Specimen after repair; (**c**) Repair mortar evaluation specimen.

3. Experiment Results and Analysis

3.1. Flexural, Compressive, and Bonding Strengths

Figure 7 presents the compressive and flexural strengths of the repair cementitious composites. In previous studies, it was known that CNTs were agglomerated by van der Waals forces within cement composites, resulting in an increase in internal voids and a decrease in the mechanical properties of the materials [36]. However, test results indicated that the increase in the mixture of S-CNT, led to the increase in the flexural and compressive strength. In particular, the strength of the SC9 specimen was measured to be higher than that of the plain specimen, in all stages. In other words, at the age of 28 days, the flexural and compressive strengths of the plain were 11.4 MPa and 65 MPa, respectively, and the SC9 specimen had a flexural strength of 12 MPa and a compressive strength of 68 MPa. Moreover, SC6 had the same level of strength as the plain specimen, and the strength of SC3 was slightly smaller than that of plain, but it was 96% of plain specimen's strength.

Due to a W/B ratio of 34%, which indicates a low proportion of water, it showed overall high compressive strength. As a result of these mechanical properties, it was estimated that CNTs impregnated with zeolite greatly reduced aggregation in the composites due to the hydrophilicity of zeolite, resulting in a filler effect in which nano-sized fine particles filled the voids and pores.

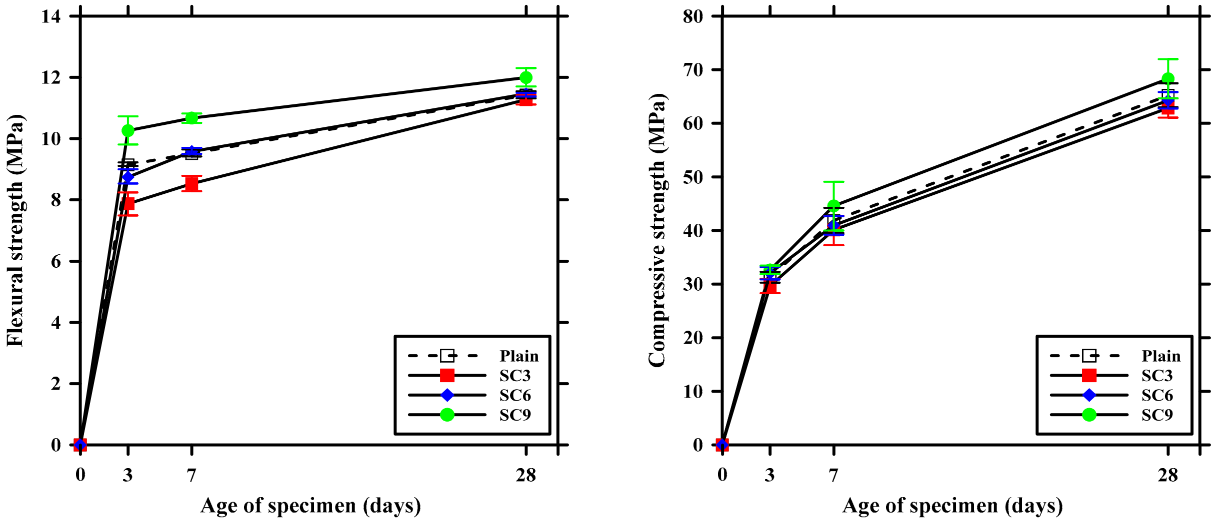

(**a**) Flexural strength (**b**) Compressive strength

Figure 7. Strength of composites: (**a**) Flexural strength; (**b**) Compressive strength.

Figure 8 exhibits the results of bonding strength of the cementitious composite. The bonding strength of repair mortar is important because it must maintain anti-corrosive performance by attaching it to the rebar exposed to the outside due to deterioration. However, in accordance with KS F 4042, the quality standard for the bonding strength between the repair mortar and the rebar is not regulated, but the bonding strength between anti-corrosive cement mortar and repair mortar, is regulated to be 1.0 MPa or higher. The results showed that the S-CNT did not reduce the bonding strength of repair mortar, compared to that of the plain specimen, and satisfied the KS standards. However, it was close to 1.0 MPa, so that it is determined that the bonding strength needs to be improved in order to secure the safety of the performance. The bonding performance of the mortar was generally determined by the unit powder amount and viscosity, and therefore it is concluded that the incorporation of S-CNT does not affect the bonding performance of the repair mortar.

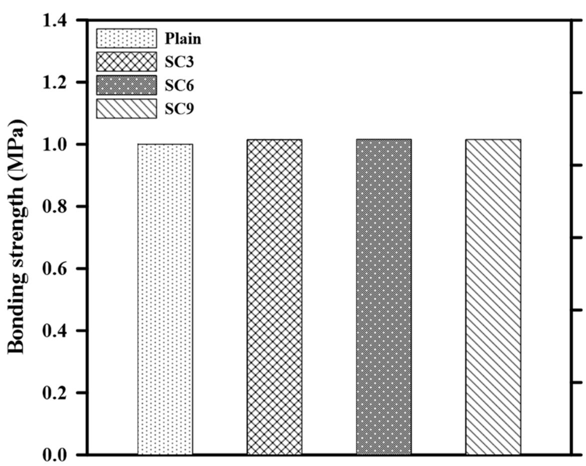

Figure 8. Bonding strength of cementitious composites.

3.2. Dry Shrinkage, Porosity, and FCR

Figure 9 presents the results of changes in dry shrinkage of the composites, according to S-CNT. First, it was found that the length of the specimen increased until the age of seven days, and this tendency was influenced by ettringite, an expansive material initially produced by the cement hydration reaction. After moving from the water curing to the environmental chamber, a rapid shrinkage was observed. The overall trend of decrease showed that the decrease rate of specimens with S-CNTs were smaller than that of the plain specimen, and the rate of change in length decreased as the amount of S-CNT increased. This tendency was due to the filler effect, in which improved dispersibility of CNT impregnated with zeolite led to the tight filling of the repair mortar. However, it was measured that the reduction rate of the length change of the SC3 specimen was similar to that of the plain specimen. These results indicated that the amount of CNT incorporated was small, and it was concluded that 6% or more of S-CNT should be incorporated in order to reduce the length change rate. The optimal dosage of 9% of mixing proportion was determined from the experimental results of the flexural and compressive strength tests, the bending strength test, and the drying shrinkage of the composites.

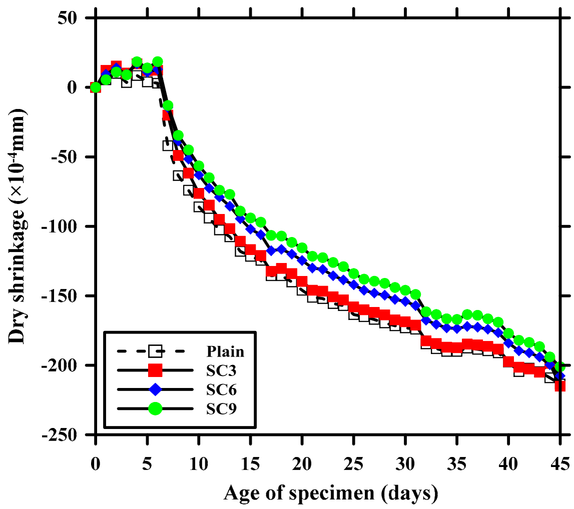

Figure 9. Change in dry shrinkage of composites according to S-CNT.

Figure 10 shows the results of comparing the pore size distribution of cementitious composite with 9% of powder CNT, and S-CNT. First of all, relatively large pores of 800~100 µm and 5~1 µm were mainly observed in the specimen with powder CNT, while the specimen with S-CNT had small pores of 1~0.05 µm. It was estimated that the test specimen mixed with powdered CNTs had larger pores due to the agglomeration of CNTs, whereas the test specimen 9% of S-CNT had improved dispersibility so that large pores did not occur. It could be concluded that these effects contributed to the improvement of the mechanical and physical properties of the repair mortar.

Figure 11 provides the results of change in FCR according to dosage of S-CNT. All of the repair mortars mixed with S-CNT showed a clear change in electrical resistance as the load was repeated, confirming the self-sensing performance. In particular, similar FCR values between 0.4 and 0.6 were measured, regardless of S-CNT incorporation. This was because conductivity was imparted to the repair composites as S-CNT was incorporated. However, the reason why FCR was not high, was that tensile and compression cracks occurred in the lower and upper parts, respectively, as the load was applied to the specimen, with the result that, as the connection distance between CNTs on the upper side became closer, it was estimated that the overall electrical resistance value of the specimen did not increase significantly. Accordingly, it was concluded that a method of measuring electrical resistance only at the lower side where tensile cracks occur, should be considered for self-sensing of the bending member.

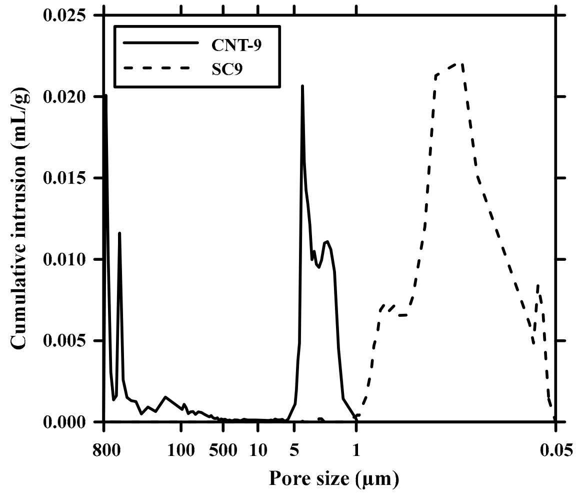

Figure 10. Pore size distribution of cementitious composites with CNT and S-CNT.

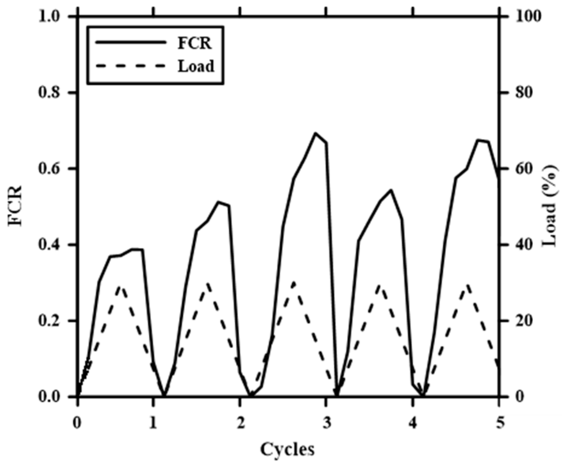

(**a**) S-CNT (3%)

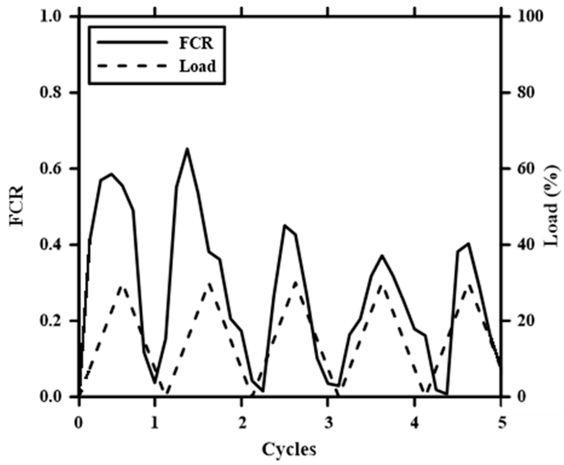

(**b**) S-CNT (6%)

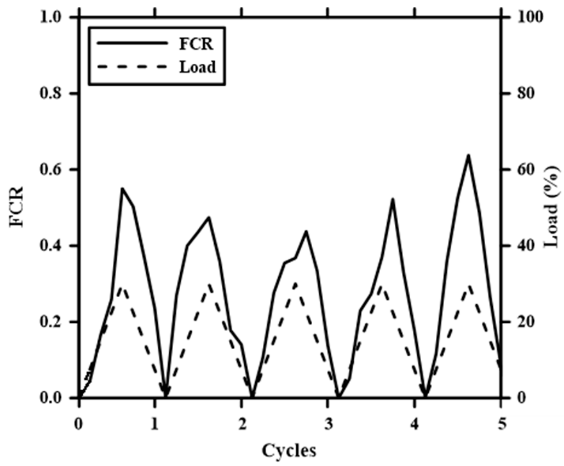

(**c**) S-CNT (9%)

Figure 11. FCR according to S-CNT: (**a**) S-CNT (3%); (**b**) S-CNT (6%); (**c**) S-CNT (9%).

3.3. Flexural Strength and FCR after Repair

Figure 12 illustrates the result of measuring the flexural strength after repairing the plate specimen with repair mortar. The flexural strength of the plate specimen was observed to be 9.8 MPa at the age of 28 days. Plain mortar and the repair mortar mixed with 9% of

S-CNT did not completely harden at the age of 3 days, so the flexural strength was much lower. The repair mortar had the same flexural strength as did the plain specimen from the age of 7 days, and it became about 14 MPa at the age of 28 days, which was measured more than 4 MPa higher than the plain specimen. It signified that the repair mortar had better performance than the plain specimen in terms of flexural strength. However, for the performance of emergency construction or immediate repair, it was concluded that the ultra-fast material should be used.

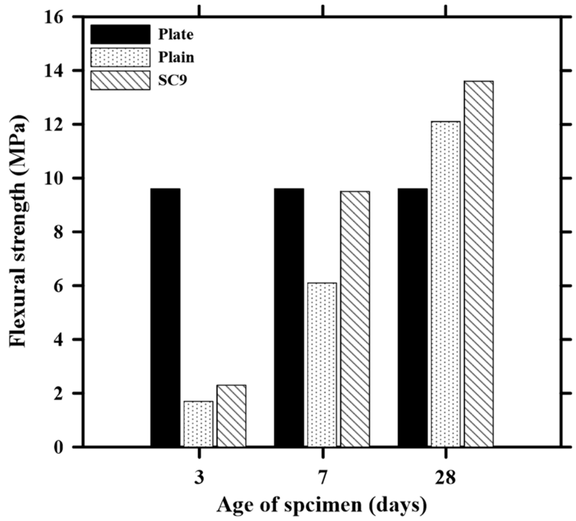

Figure 12. Flexural strength after application of repair composites.

Figure 13 shows fractural change in electrical resistance applied with repair materials. As a result of the experiment, it was observed that the FCR was clearly detected according to the cyclic loading. In particular, the electricity resistance range was between 0 and 2.0%, which was higher than FCR with S-CNT. When a bending load was applied, tensile cracks were preferentially generated in the lower part of the specimen. As tensile cracks occurred in the lower part repaired with the composites, the rate of change in electrical resistance was definitely higher. Therefore, it was concluded that it can be applied to the lower part of the existing beam member requiring self-sensing.

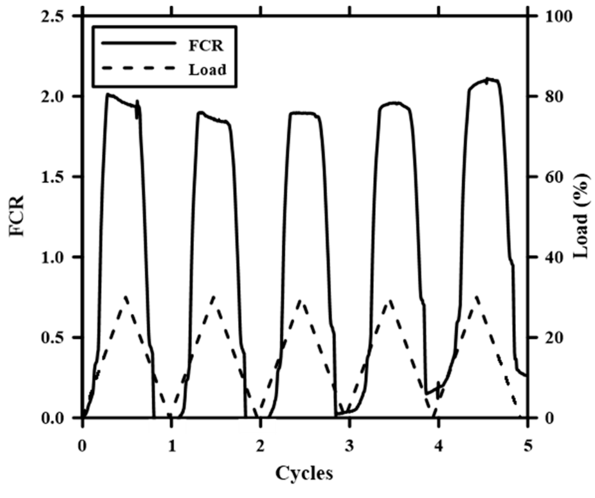

Figure 13. FCR applied with repair material.

4. Conclusions

In this paper, first, CNT-impregnated porous powder, which was called S-CNT, was produced, using the porous powder zeolite. Repair self-sensing composites based on S-

CNT were made and their mechanical, electrical, and repair performances were evaluated through several experiments, and the following conclusions eventually were reached.

- An impregnation process with MWCNT and porous powder was proposed and the powder form, called S-CNT, was investigated using SEM. CNT impregnated with zeolite, which is a porous material, was not inserted into the pores of the zeolite but was attached to the surface, because it was estimated that both the diameters of the zeolite pores and the CNTs were nano-sized, such that CNT was hard to insert into the pores of the zeolite.
- The strength of the repair mortar mixed with S-CNT was measured to increase as the mixing ratio increased. In particular, flexural and compressive strength of the SC9 specimen at the age of the 28 days, was observed to be 105% greater than those of plain specimen. This is because the CNTs attached to the hydrophilic zeolite surface were homogeneously dispersed in the composites, and the internal voids were reduced by the filler effect. It was also confirmed that relatively large pores of 800 to 360 μm, and 10 to 1 μm, were reduced when measuring the pore size distribution, and it was measured that the drying shrinkage was also reduced. The results of the bonding strength test indicated that the bonding strength satisfied the KS standard of 1.0 MPa, and it was concluded that there was no significant effect on the bonding strength according to the S-CNT incorporation. The FCRs of the composites under repeated load were measured to confirm the self-sensing performance, and it was found that all sensing performance was secured by the incorporation of S-CNT.
- Based on the experimental results of the flexural and compressive strength tests, bonding strengths, drying shrinkages, and FCRs, the optimal dosage of mixing proportion was 9%, so that only SC9 was used for the flexural and FCR tests with the repair composites. The result of the flexural test indicated that the repair mortar had better performance than the plain after the age of seven days. However, for the performance of emergency construction or immediate repair part, it was impossible to use the composites, because their early strengths were much lower than that of the plain specimen, such that ultra-fast material should be used. Moreover, it was clearly measured that the FCRs of the composites after repair were detected according to the cyclic loading. In particular, the electricity resistance ranges were measured from 0 to 2.0%, which were higher than the FCRs of SC3, SC6, and SC9. It was found that it can be used in the lower part of the beam requiring self-sensing.
- The proposed repair self-sensing composites improved the dispersion performance degradation of CNTs due to van der Waals forces. The proposed repair self-sensing material can provide basic information that can be used to evaluate the soundness of a building, after using it to repair existing structures.

Author Contributions: Y.K.: data curation, writing—original draft preparation; S.-Y.S.: Writing—review and editing, project administration, funding acquisition; H.-D.Y.: Writing—review and editing, project administration, funding acquisition; G.-C.L.: Conceptualization, methodology, formal analysis, resources, data curation, writing—review and editing, supervision, project administration, funding acquisition; S.H.: Formal analysis, writing—original draft preparation, writing—review and editing, visualization, supervision. All authors have read and agreed to the published version of the manuscript.

Funding: This research was supported by the Basic Science Research Program through the National Research Foundation of Korea (NRF), funded by the Ministry of Education (No. 2020R1F1A1048241 and 2021R1A4A2001964). The views expressed are those of authors, and do not necessarily represent those of the sponsors.

Data Availability Statement: The datasets used and analyzed in this study are all included in the manuscript, figures, and tables.

Conflicts of Interest: The authors declare that they have no known competing financial interests or personal relationships that could have appeared to influence the work reported in this paper.

References

1. Sharma, S.; Dangi, S.K.; Bairwa, S.K.; Sen, S. Comparative study on sensitivity of acceleration and strain responses for bridge health monitoring. *J. Struct. Integr. Maint.* **2022**, *4*, 238–251. [CrossRef]
2. Balageas, D.; Fritzen, C.P.; Güemes, A. *Structural Health Monitoring*, 1st ed.; Wiley-ISTE: London, UK, 2010.
3. Mitra, M.; Gopalakrishnan, S. Guided wave based structural health monitoring: A review. *Smart Mater. Struct.* **2016**, *25*, 053001. [CrossRef]
4. Yan, R.; Chen, X.; Mukhopadhyay, S.C. *Structural Health Monitoring*, 1st ed.; Springer: Berlin/Heidelberg, Germany, 2017.
5. Colombani, I.A.; Andrawes, B. A study of multi-target image-based displacement measurement approach for field testing of bridges. *J. Struct. Integr. Maint.* **2022**, *1*, 207–216. [CrossRef]
6. Bao, Y.; Chen, Z.; Wei, S.; Xu, Y.; Tang, Z.; Li, H. The state of the art of data science and engineering in structural health monitoring. *Engineering* **2019**, *5*, 234–242. [CrossRef]
7. Wang, C.S.; Wu, F.; Chang, F.K. Structural health monitoring from fiber-reinforced composites to steel-reinforced concrete. *Smart Mater. Struct.* **2001**, *10*, 548–552.
8. Wen, S.; Chung, D.D.L. Electrical-resistance-based damage self-sensing in carbon fiber reinforced cement. *Carbon* **2007**, *45*, 710–716. [CrossRef]
9. Sedkova, L.; Vik, V.; Sedek, J. Delamination/disbond propagation analysis in adhesively bonded composite joints using guided waves. *J. Struct. Integr. Maint.* **2022**, *7*, 25–33.
10. Azhari, F.; Banthia, N. Cement-based sensors with carbon fibers and carbon nanotubes for piezo resistive sensing. *Cem. Concr. Compos.* **2012**, *34*, 866–873. [CrossRef]
11. Galao, O.; Baeza, F.J.; Zornoza, E.; Garcés, P. Strain and damage sensing propertieson multifunctional cement composites with CNF admixture. *Cem. Concr. Compos.* **2014**, *46*, 90–98. [CrossRef]
12. Kim, H.K.; Park, I.S.; Lee, H.K. Improved piezo resistive sensitivity and stability of CNT/cement mortar composites with low water–binder ratio. *Compos. Struct.* **2014**, *116*, 713–719. [CrossRef]
13. Lee, S.J.; You, I.; Zi, G.; Yoo, D.Y. Experimental investigation of the piezo resistive properties of cement composites with hybrid carbon fibers and nanotubes. *Sensor* **2017**, *17*, 2516. [CrossRef] [PubMed]
14. Yoo, D.Y.; You, I.; Lee, S.J. Electrical properties of cement-based composites with carbon nanotube, graphene, and graphite nanofiber. *Sensor* **2017**, *17*, 1064. [CrossRef] [PubMed]
15. Zhou, C.; Li, F.; Hu, J.; Ren, M.; Wei, J.; Yu, Q. Enhanced mechanical properties of cement paste by hybrid graphene oxide/carbon nanotubes. *Constr. Build. Mater.* **2017**, *1314*, 336–345. [CrossRef]
16. You, I.; Yoo, D.Y.; Kim, S.; Kin, M.J.; Zi, G. Elctrical and Self-Sensing Properties of Ultra-High-Performance Fiber-Reinforced Concrete with Carbon Nanotubes. *Sensor* **2017**, *17*, 2481. [CrossRef] [PubMed]
17. Yoo, D.Y.; You, I.; Youn, H.; Lee, S.J. Electrical and piezo resistive properties of cement composites with carbon nanomaterials. *J. Compos. Mater.* **2018**, *52*, 3325–3340. [CrossRef]
18. Dong, W.; Li, W.; Shen, L.; Sheng, D. Piezo resistive behaviours of carbon black cement-based sensors with layer-distributed conductive rubber fibres. *Mater. Des.* **2019**, *182*, 108012. [CrossRef]
19. Kim, G.M.; Nam, I.W.; Yang, B.; Yoon, H.N.; Lee, H.K.; Park, S. Carbon nanotube (CNT) incorporated cementitious composites for functional construction materials: The state of the art. *Compos. Struct.* **2019**, *227*, 111244. [CrossRef]
20. Nayak, S.; Das, S. A microstructure-guided numerical approach to evaluate strain sensing and damage detection ability of random heterogeneous self-sensing structural materials. *Comput. Mater. Sci.* **2019**, *156*, 195–205. [CrossRef]
21. Rovnaník, P.; Kusak, I.; Bayer, P.; Schmid, P.; Fiala, L. Comparison of electrical and self-sensing properties of Portland cement and alkali-activated slag mortars. *Cem. Concr. Res.* **2019**, *118*, 84–91. [CrossRef]
22. Suchorozewski, J.; Prieto, M.; Mueller, U. An experimental study of self-sensing concrete enhanced with multiwall carbon nanotubes in wedge splitting test and DIC. *Constr. Build. Mater.* **2020**, *262*, 120871. [CrossRef]
23. Abebi, M.; Fangueiro, R.; Correia, A.G. Effects of multiscale carbon-based conductive fillers on the performances of a self-sensing cementitious geocomposite. *J. Build. Eng.* **2021**, *43*, 103171. [CrossRef]
24. Dinesh, A.; Sudharan, S.T.; Haribala, S. Self-sensing cement-based sensor with carbon nanotube: Fabrication and properties—A review. *Mater. Today Proc.* **2021**, *46*, 5801–5807. [CrossRef]
25. Lee, S.J.; Lee, J.E.; Dinh, N.H.; Choi, K.K. Time history analysis for investigation of dynamic behavioral characteristics of uninterruptible power supply system. *J. Struct. Integr.* **2022**, *7*, 91–109. [CrossRef]
26. Lee, H.; Yu, W.; Chung, W. Damage Detection of Carbon Nanotube Cementitious Composites Using Thermal and Electrical Resistance Properties. *Appl. Sci.* **2021**, *11*, 2955. [CrossRef]
27. Yu, J.; Grossiord, N.; Koning, C.E.; Loos, J. Controlling the dispersion of multi-wall carbon nanotubes in aqueous surfactant solution. *Carbon* **2007**, *45*, 618–623. [CrossRef]
28. Ma, P.-C.; Siddiqui, N.A.; Marom, G.; Kim, J.-K. Dispersion and functionalization of carbon nanotubes for polymer-based nanocomposites: A review. *Compos. Part A Appl. Sci. Manuf.* **2010**, *41*, 1345–1367. [CrossRef]
29. Makar, J.M.; Margeson, J.C.; Luh, J. Carbon nanotube/cement composites-early results and potential applications. In Proceedings of the 3rd International Conference on Construction Materials: Performance, Innovations and Structural Implications, Vancouver, BC, Canada, 22–24 August 2005; pp. 1–10.

30. Konsta-Gdoutos, M.S.; Metaxa, Z.S.; Shah, S.P. Multi-scale mechanical and fracture characteristics and early-age strain capacity of high performance carbon nanotube/cement nanocomposites. *Cem. Concr. Compos.* **2010**, *32*, 110–115. [CrossRef]
31. Luo, Y.; Heng, Y.; Dai, X.; Chen, W.; Li, J. Preparation and photocatalytic ability of highly defective carbon nanotubes. *J. Solid State Chem.* **2009**, *182*, 2521–2525. [CrossRef]
32. Kim, B.R.; Lee, H.K.; Kim, E.; Lee, S.H. Intrinsic electromagnetic radiation shielding/absorbing characteristics of polyaniline-coated transparent thin films. *Synth. Met.* **2010**, *160*, 1838–1842. [CrossRef]
33. Cwirzen, A.; Habermehl-Cwirzen, K.; Penttala, V. Surface decoration of carbon nanotubes and mechanical properties of cement/carbon nanotube composites. *Adv. Cem. Res.* **2008**, *20*, 65–73. [CrossRef]
34. Nochaiya, T.; Chaipanich, A. Behavior of multi-walled carbon nanotubes on the porosity and microstructure of cement-based materials. *Appl. Surf. Sci.* **2011**, *257*, 1941–1945. [CrossRef]
35. Madenci, E.; Özkılıç, Y.O.; Aksoylu, C.; Asyraf, M.R.M.; Syamsir, A.; Supian, A.B.M.; Elizaveta, B. Experimental and Analytical Investigation of Flexural Behavior of Carbon Nanotube Reinforced Textile Based Composites. *Materials* **2023**, *16*, 2222. [CrossRef] [PubMed]
36. Lee, G.C.; Kim, Y.; Hong, S. Influence of powder and liquid multi-wall carbon nanotube on hydration and dispersion of the cementitious composites. *Appl. Sci.* **2020**, *10*, 7948. [CrossRef]